Image and Vision Computing 25(4):455–463, 2007 (ISMM05 special issue) – ©Elsevier B.V. 2007

Theoretical Foundations for Spatially Discrete 1-D Shock Filtering

Martin Welk, Joachim Weickert, Irena Galić

Mathematical Image Analysis Group, Faculty of Mathematics and Computer Science,
Bldg. E11, Saarland University, 66041 Saarbrücken, Germany
{welk, weickert, galic}@mia.uni-saarland.de

Abstract

While shock filters are popular morphological image enhancement methods, no well-posedness theory is available for their corresponding partial differential equations (PDEs). By analysing the dynamical system of ordinary differential equations that results from a space discretisation of a PDE for 1-D shock filtering, we derive an analytical solution and prove well-posedness. We show that the results carry over to the fully discrete case when an explicit time discretisation is applied. Finally we establish an equivalence result between discrete shock filtering and local mode filtering.

Keywords: Shock filters, analytical solution, well-posedness, dynamical systems, mode filters

1 Introduction

Shock filters are morphological image enhancement methods where dilation is performed around maxima and erosion around minima. Iterating this process leads to a segmentation with piecewise constant segments that are separated by discontinuities, so-called shocks. This makes shock filtering attractive for a number of applications where edge sharpening and a piecewise constant segmentation is desired.

In 1975 the first shock filters have been formulated by Kramer and Bruckner in a fully discrete manner [8], while first continuous formulations by means of partial differential equations (PDEs) have been developed in 1990 by Osher and Rudin [10]. The relation of these methods to the discrete Kramer–Bruckner filter became clear several years later [6, 14]. PDE-based shock filters have been investigated in a number of papers. Many of them proposed modifications with higher robustness under noise [1, 4, 7, 9, 14], but also coherence-enhancing shock filters [19] and numerical schemes have been studied [13].

Let us consider some continuous d-dimensional initial image $f : \mathbb{R}^d \to \mathbb{R}$. In the simplest case of a PDE-based shock filter [10], one obtains a filtered version $u(x,t)$ of $f(x)$ by solving the evolution equation

$$\partial_t u = -\operatorname{sgn}(\Delta u)\,|\nabla u| \qquad (t \geq 0)$$

with f as initial condition, i.e. $u(x,0) = f(x)$. Experimentally one observes that within finite "evolution time" t, a piecewise constant, segmentation-like result is obtained (see Fig. 1).

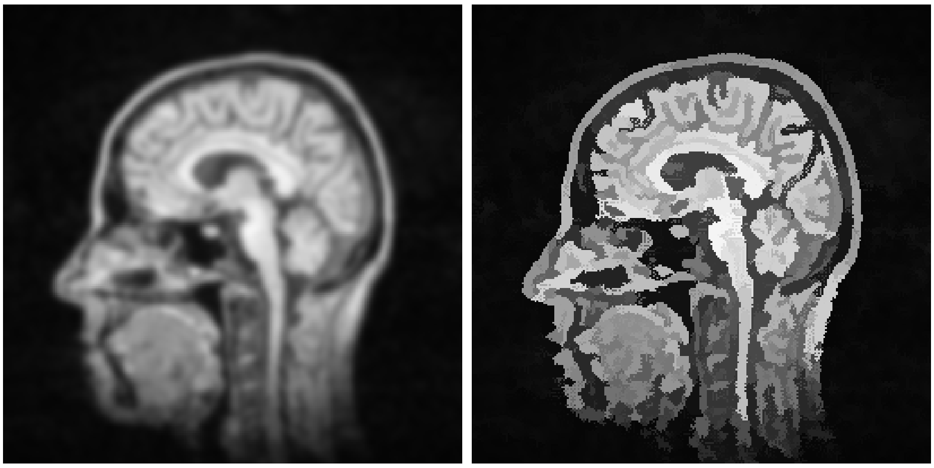

Figure 1: LEFT: Original image. RIGHT: After applying the Osher–Rudin shock filter.

Specialising to the one-dimensional case, we obtain

$$\partial_t u = -\operatorname{sgn}(\partial_{xx} u)\,|\partial_x u| = \begin{cases} |\partial_x u|\,, & \partial_{xx} u < 0, \\ -\,|\partial_x u|\,, & \partial_{xx} u > 0, \\ 0, & \partial_{xx} u = 0. \end{cases} \tag{1}$$

It is clearly visible that this filter performs dilation $\partial_t u = |\partial_x u|$ in concave segments of u, while in convex parts the erosion process $\partial_t u = -\,|\partial_x u|$ takes place. The time t specifies the radius of the interval (a 1-D disk) $[-t, t]$ as structuring element. For a derivation of these PDE formulations for classical morphological operations, see e.g. [2].

While there is clear experimental evidence that shock filtering is a useful operation, no analytical solutions and well-posedness results are available for PDE-based shock filters. In general this problem is considered to be too difficult, since shock filters have some connections to classical ill-posed problems such as backward diffusion [10, 9].

The main goal of the present paper is to show that it is possible to establish analytical solutions and well-posedness as soon as we study the *semidiscrete* case with a spatial discretisation and a continuous time parameter t. This case is of great practical relevance, since digital images already induce a natural space discretisation. For the sake of simplicity we restrict ourselves to the 1-D case. We also show that these results carry over to the fully discrete case with an explicit (Euler forward) time discretisation, and we establish an equivalence result between shock filtering and a specific image enhancement method called mode filtering.

Our paper is organised as follows: In Section 2 we present an analytical solution and a well-posedness proof for the semidiscrete case, whereas corresponding fully discrete results are given in Section 3. An equivalence result between shock and mode filters is presented in Section 4, and the paper is concluded with a summary in Section 5.

A shorter version of the current paper appeared at the *2005 International Symposium on Mathematical Morphology* [20]. The present paper extends these results by investigations on signals with linear pixels and by establishing an equivalence between shock and mode filters.

2 The Semidiscrete Model

2.1 Problem Statement

In this section, we are concerned with a spatial discretisation of (1) which we will describe now. The time variable remains continuous here. Throughout the paper, the notion *semidiscrete* will refer to this setting.

Problem. *Let $(\ldots, u_0(t), u_1(t), u_2(t), \ldots)$ be a time-dependent bounded real-valued signal which evolves according to*

$$\dot{u}_i = \begin{cases} \max(u_{i+1} - u_i, u_{i-1} - u_i, 0), & 2u_i > u_{i+1} + u_{i-1}, \\ \min(u_{i+1} - u_i, u_{i-1} - u_i, 0), & 2u_i < u_{i+1} + u_{i-1}, \\ 0, & 2u_i = u_{i+1} + u_{i-1} \end{cases} \tag{2}$$

with the initial conditions

$$u_i(0) = f_i. \tag{3}$$

Assume further that the signal is either of infinite length with compact support, or finite with reflecting boundary conditions.

Here, $\dot{u}_i$ denotes the time derivative of $u_i(t)$. Like (1), this filter switches between dilation and erosion depending on the local convexity or concavity of the signal. Dilation and erosion themselves are modeled by upwind-type discretisations [11], which are well established for dilation and erosion PDEs because they guarantee the detection of local extrema and stabilise the discretised process by adapting the discrete representation to the local directedness of the PDE evolution.

It should be noted that in case $2u_i > u_{i+1} + u_{i-1}$ the two neighbour differences $u_{i+1} - u_i$ and $u_{i-1} - u_i$ cannot be simultaneously positive; with the opposite inequality they cannot be simultaneously negative. In fact, always when the maximum or minimum in (2) does not select its third argument, zero, it returns the absolutely smaller of the neighbour differences.

No modification of (2) is needed for finite-length signals with reflecting boundary conditions. In this case, each boundary pixel has one vanishing neighbour difference.

In order to study the solution behaviour of this system, we have to specify the possible solutions, taking into account that the right-hand side of (2) may involve discontinuities. We call a time-dependent signal $u(t) = (\ldots, u_1(t), u_2(t), u_3(t) \ldots)$ a *solution* of (2) if

(I) each u_i is a piecewise differentiable function of t,

(II) each u_i satisfies (2) for all times t for which $\dot{u}_i(t)$ exists,

(III) for $t = 0$, the right-sided derivative $\dot{u}_i^+(0)$ equals the right-hand side of (2) if $2u_i(0) \neq u_{i+1}(0) + u_{i-1}(0)$.

We also remark that throughout this paper, extremality of pixels is handled strictly local: A pixel u_i of a 1-D space-discrete signal u is called a local extremum whenever $(u_i - u_{i-1})(u_{i+1} - u_i) \leq 0$. For example, in the sequence of five pixels $u_1 > u_2 = u_3 = u_4 > u_5$, pixels u_2 and u_3 are local minima while u_3 and u_4 are local maxima.

2.2 Well-Posedness Results

The following theorem contains our main result.

Theorem 2.1 (Well-Posedness) *For our Problem, assume that the equality $f_{k+1} - 2f_k + f_{k-1} = 0$ does not hold for any pixel f_k which is not a local maximum or minimum of f. Then the following are true:*

(i) ***Existence and uniqueness:*** *The Problem has a unique solution for all $t \geq 0$.*

(ii) ***Maximum–minimum principle:*** *If there are real bounds a, b such that $a < f_k < b$ holds for all k, then $a < u_k(t) < b$ holds for all k and all $t \geq 0$.*

(iii) l_∞***-stability:*** *There exists a $\delta > 0$ such that for any initial signal $\tilde{f}$ with $\|\tilde{f} - f\|_\infty < \delta$ the corresponding solution $\tilde{u}$ satisfies the inequality*

$$\|\tilde{u}(t) - u(t)\|_\infty < \|\tilde{f} - f\|_\infty$$

for all $t > 0$. The solution therefore depends l_∞-continuously on the initial conditions within a neighbourhood of f.

(iv) ***Total variation preservation:*** *If the total variation of f is finite, then the total variation of u at any time $t \geq 0$ equals that of f.*

(v) ***Steady state:*** *For $t \to \infty$, the signal u converges to a piecewise constant signal. The jumps in this signal are located at the steepest slope positions of the original signal.*

All statements of this theorem follow from an explicit analytical solution of the Problem that will be described in the following proposition.

Proposition 2.2 (Analytical Solution) *For our Problem, let the segment $(f_1, \ldots, f_m)$ be strictly decreasing and concave in all pixels. Assume that the leading pixel f_1 is either a local maximum or a neighbour to a convex pixel $f_0 > f_1$. Then the following hold for all $t \geq 0$:*

(i) If f_1 is a local maximum of f, $u_1(t)$ is a local maximum of $u(t)$.

(ii) If f_1 is neighbour to a convex pixel $f_0 > f_1$, then $u_1(t)$ also has a convex neighbour pixel $u_0(t) > u_1(t)$.

(iii) The segment $(u_1, \ldots, u_m)$ remains strictly decreasing and concave in all pixels. The grey values of all pixels at time t are given by

$$\begin{aligned} u_k(t) = C \cdot & \left(1 + (-1)^k \mathrm{e}^{-2t} - \mathrm{e}^{-t} \sum_{j=0}^{k-2} \frac{t^j}{j!}\left(1 + (-1)^{k-j}\right)\right) \\ & + \mathrm{e}^{-t} \sum_{j=0}^{k-2} \frac{t^j}{j!} f_{k-j} - (-1)^k f_1 \mathrm{e}^{-t} \left(\mathrm{e}^{-t} - \sum_{j=0}^{k-2} \frac{(-t)^j}{j!}\right) \end{aligned} \tag{4}$$

for $k = 1, \ldots, m$, where $C = f_1(0)$ if f_1 is a local maximum of f, and $C = \frac{1}{2}(f_0(0) + f_1(0))$ otherwise.

(iv) At no time $t \geq 0$, the equation $2u_i(t) = u_{i+1}(t) + u_{i-1}(t)$ becomes true for any $i \in \{1, \dots, m\}$.

Analogous statements hold for increasing concave and for convex signal segments.

In a signal that contains no locally linear pixels (such with $2f_i = f_{i+1} + f_{i-1}$), each pixel belongs to a chain of either concave or convex pixels led by an extremal pixel or an "inflection pair" of a convex and a concave pixel. Therefore Proposition 2.2 completely describes the dynamics of such a signal. Let us prove this proposition.

Proof. We show in steps 1.–3. that the claimed evolution equations hold as long as the initial monotonicity and convexity properties of the signal segment prevail. Step 4. then completes the proof by demonstrating that the evolution equations preserve exactly these monotonicity and convexity requirements.

1. From (2) it is clear that any pixel u_i which is extremal at time t has $\dot{u}_i(t) = 0$ and therefore does not move. Particularly, if f_1 is a local maximum of f, then $u_1(t)$ remains constant as long as it continues to be a maximum.

2. If $u_0 > u_1$, u_0 is convex and u_1 concave for $t \in [0, T)$. Then we have for these pixels

$$\begin{aligned} \dot{u}_0 &= u_1 - u_0 \;, \\ \dot{u}_1 &= u_0 - u_1 \;, \end{aligned} \tag{5}$$

which by the substitutions $y := \frac{1}{2}(u_0 + u_1)$ and $v := u_1 - u_0$ becomes

$$\begin{aligned} \dot{y} &= 0 \;, \\ \dot{v} &= -2v \;. \end{aligned}$$

This system of linear ordinary differential equations (ODEs) has the solution $y(t) = y(0) = C$ and $v(t) = v(0)\exp(-2t)$. Backsubstitution gives

$$\begin{aligned} u_0(t) &= C \cdot (1 - \mathrm{e}^{-2t}) + f_0 \mathrm{e}^{-2t} \;, \\ u_1(t) &= C \cdot (1 - \mathrm{e}^{-2t}) + f_1 \mathrm{e}^{-2t} \;. \end{aligned} \tag{6}$$

This explicit solution is valid as long as the convexity and monotonicity properties of u_0 and u_1 do not change.

3. Assume the monotonicity and convexity conditions required by the proposition for the initial signal hold for $u(t)$ for all $t \in [0, T)$. Then we have in all cases, defining C as in the proposition, the system of ODEs

$$\begin{aligned} \dot{u}_1 &= -2(u_1 - C) \;, \\ \dot{u}_k &= u_{k-1} - u_k \;, \qquad k = 2, \dots, m \end{aligned} \tag{7}$$

for $t \in [0, T)$. We substitute further $v_k := u_k - C$ for $k = 1, \dots, m$ as well as $w_1 := v_1$ and $w_k := v_k + (-1)^k v_1$ for $k = 2, \dots, m$. This leads to the system

$$\begin{aligned} \dot{w}_1 &= -2w_1 \;, \\ \dot{w}_2 &= -w_2 \;, \\ \dot{w}_k &= w_{k-1} - w_k \;, \qquad k = 3, \dots, m \;. \end{aligned} \tag{8}$$

This system of linear ODEs has the unique solution

$$w_1(t) = w_1(0)\mathrm{e}^{-2t} \ ,$$
$$w_k(t) = \mathrm{e}^{-t} \sum_{j=0}^{k-2} \frac{t^j}{j!} w_{k-j}(0) \ , \qquad k = 2, \ldots, m$$

which after reverse substitution yields (4) for all $t \in [0, T]$.
4. Note that (5) and (7) are systems of linear ODEs which have the unique explicit solutions (6) and (4) for all $t > 0$. As long as the initial monotonicity and convexity conditions are satisfied, the solutions of (2) coincide with those of the linear ODE systems.

We prove therefore that the solution (4) fulfils the monotonicity condition

$$u_k(t) - u_{k-1}(t) < 0 \ , \qquad k = 2, \ldots, m \ ,$$

and the concavity conditions

$$u_{k+1}(t) - 2u_k(t) + u_{k-1}(t) < 0 \ , \qquad k = 1, \ldots, m \ ,$$

for all $t > 0$ if they are valid for $t = 0$. To see this, we calculate first

$$u_k(t) - u_{k-1}(t) = \mathrm{e}^{-t} \sum_{j=0}^{k-2} \frac{t^j}{j!} (f_{k-j} - f_{k-1-j}) + 2\mathrm{e}^{-t}(-1)^{k-1} \left(\mathrm{e}^{-t} - \sum_{j=0}^{k-2} \frac{(-t)^j}{j!} \right) (f_1 - C) \ .$$

By hypothesis, $f_{k-j} - f_{k-1-j}$ and $f_1 - C$ are negative. Further, $\exp(-t) - \sum_{j=0}^{k-2} (-t)^j / j!$ is the error of the (alternating) Taylor series of $\exp(-t)$, thus having the same sign $(-1)^{k-1}$ as the first neglected member. Consequently, monotonicity is preserved by (4) for all $t > 0$.

Second, we have for $k = 2, \ldots, m-1$

$$\begin{aligned} u_{k+1}(t) - 2u_k(t) + u_{k-1}(t) = {} & \mathrm{e}^{-t} \sum_{j=0}^{k-2} \frac{t^j}{j!} (f_{k-j+1} - 2f_{k-j} + f_{k-j-1}) \\ & + 4\mathrm{e}^{-t}(-1)^k \left(\mathrm{e}^{-t} - \sum_{j=0}^{k-1} \frac{(-t)^j}{j!} \right) (f_1 - C) \\ & + \mathrm{e}^{-t} \frac{t^{k-1}}{(k-1)!} (f_2 - 3f_1 + 2C) \end{aligned}$$

which is seen to be negative by similar reasoning as above.

Concavity at $u_m(t)$ follows in nearly the same way. By extending (4) to $k = m+1$, one obtains not necessarily the true evolution of u_{m+1} since that pixel is not assumed to be included in the concave segment. However, the true trajectory of u_{m+1} can only lie below or on that predicted by (4).

Third, if f_1 is a maximum of f, then $u_1(t)$ remains one for all $t > 0$ which also ensures concavity at u_1. If f_1 has a convex neighbour pixel $f_0 > f_1$, we have instead

$$u_2(t) - 2u_1(t) + u_0(t) = \mathrm{e}^{-t}(f_2 - 2f_1 + f_0) + 4\mathrm{e}^{-t}(1 - \mathrm{e}^{-t})(f_1 - C) < 0$$

which is again negative for all $t > 0$.

Finally, we remark that the solution (6) ensures $u_0(t) > u_1(t)$ for all $t > 0$ if it holds for $t = 0$. That convexity at u_0 is preserved can be established by analogous reasoning as for the concavity at u_1.

Since the solutions from the linear systems guarantee preservation of all monotonicity and convexity properties which initially hold for the considered segment, these solutions are the solutions of (2) for all $t > 0$. □

Proof of Theorem 2.1. Existence and uniqueness of the solution follow from the proof of Proposition 2.2.

The maximum–minimum principle and preservation of total variation follow from the fact that extrema do not move, and monotonicity is preserved for all $t > 0$. Note that by the specification of our Problem, each non-extremal pixel in the signal belongs to a segment enclosed by two extrema.

For the l_∞-stability, note that for each admissible initial signal f, there exists a lower bound $\gamma > 0$ for all values of $|f_{k-1} - f_k|$ which are not zero, and a lower bound $\eta > 0$ for all values of $|f_{k-1} - 2f_k + f_{k+1}|$ for pixels k which are not local extrema of f. Let a signal $\tilde{f}$ with $\|\tilde{f} - f\|_\infty =: d < \min\{\gamma/2, \eta/4\}$ be given. One easily checks that then the monotonicity and convexity properties of all strictly monotone segments of f are preserved in $\tilde{f}$. Moreover, isolated extremal pixels of f will be such in $\tilde{f}$. Only chains of equal pixels $f_k = \ldots = f_{k+l}$ may break up in $\tilde{f}$, but in this case the corresponding chain $\tilde{f}_k, \ldots, \tilde{f}_{k+l}$ contains at least one extremum or one inflection pair. To sum up, each monotone and convex/concave segment in f with one of the pixels $f_k = \ldots = f_{k+l}$ as leading pixel is turned into a segment of equal character in $\tilde{f}$ whose leading pixel is one of $\tilde{f}_k, \ldots, \tilde{f}_{k+l}$.

Let us choose without loss of generality a pixel $\tilde{f}_k$ within a decreasing and concave segment as in the proposition. By virtue of $|\tilde{C} - C| \le d$ and $|\tilde{f}_j - f_j| \le d$, we can estimate the difference of the explicit solutions (4) for $\tilde{u}_k$ and u_k:

$$
\begin{aligned}
|\tilde{u}_k(t) - u_k(t)| \le d \cdot \Bigg(& \left| 1 - \mathrm{e}^{-t} \sum_{j=0}^{k-2} \frac{t^j}{j!} + (-1)^k \mathrm{e}^{-t} \left(\mathrm{e}^{-t} - \sum_{j=0}^{k-2} \frac{(-t)^j}{j!} \right) \right| \\
& + \mathrm{e}^{-t} \sum_{j=0}^{k-2} \frac{t^j}{j!} + \mathrm{e}^{-t} \cdot \left| \mathrm{e}^{-t} - \sum_{j=0}^{k-2} \frac{(-t)^j}{j!} \right| \Bigg) \\
\le d &
\end{aligned}
$$

which proves the l_∞-stability statement with $\delta := \min\{\gamma/2, \eta/4\}$.

Finally, the convergence to a steady state is obvious from the exponential decay of all summands but C in (4). □

The fact that the signal reaches its steady state only for $t \to \infty$ stands in contrast to the behaviour of space-continuous dilation and erosion where extrema propagate in space with constant speed. In our semidiscrete setting, non-extremal pixels only asymptotically approach their limit values. This can be seen as a blurring, or approximation error, which is the price for the performed spatial discretisation.

2.3 Signals With Linear Pixels

Our well-posedness statements in the previous section explicitly exclude signals which contain pixels f_k with $f_{k+1} - 2f_k + f_{k-1} = 0$. For brevity, we shall call such pixels *non-extremal linear pixels.*

As we are going to demonstrate, no uniqueness and continuous dependence on initial condition holds for initial signals f with non-extremal linear pixels. First of all, condition (III) allows the right-sided time derivative of such a pixel at $t = 0$ to deviate from the right-hand side of equation (2). Without this relaxation, the condition would in many cases stand in contradiction to the uniquely determined evolution of non-linear surrounding pixels, preventing the existence of solutions.

While the evolution of the neighbours of a non-extremal linear pixel will often force it to become convex or concave, this process is never unique: Instead, one can label each non-extremal linear pixel at $t = 0$ *arbitrarily* to impose either convexity or concavity. Whatever labelling is chosen, it leads to a consistent evolution for $t > 0$ in which no linear pixels reappear. This is precised in the following proposition.

Proposition 2.3 (Forking Solutions at Linear Pixels) *Let an initial signal* $f = (\ldots, f_1, f_2, f_3, \ldots)$ *be given. Let for each non-extremal linear pixel* f_k *a sign* $\sigma_k \in \{+1, -1\}$ *be chosen. Then there exists a unique solution of* (2) *in the sense of (I)–(III) with initial conditions* (3) *such that for each non-extremal linear pixel* f_k*, the right-sided derivative of* u_k *at* $t = 0$ *is*

$$\dot{u}_k^+(0) = \begin{cases} \max(u_{i+1} - u_i, u_{i-1} - u_i, 0) \ , & \sigma_k = +1 \ , \\ \min(u_{i+1} - u_i, u_{i-1} - u_i, 0) \ , & \sigma_k = -1 \ . \end{cases}$$

For none of these solutions, non-extremal linear pixels exist in $u(t)$ *for* $t > 0$.

As there is no "natural" labelling of linear pixels as convex or concave, this proposition expresses that for initial signals with non-extremal linear pixels, the spatially discrete shock filter is highly nonunique. Moreover, for such initial signals the solutions no longer depend continuously on the initial conditions: Considering a non-extremal linear pixel f_k in a signal f, it is clear that every neighbourhood of f will contain signals $\tilde{f}$ in which $\tilde{f}_k$ is strictly convex, and such in which it is strictly concave.

Proof. Assume we are given a fixed choice of the σ_k. Interpreting non-extremal linear pixels with $\sigma_k = +1$ as convex and such with $\sigma_k = -1$ as concave, we have again a segmentation of the entire signal into concave and convex regions as for signals without non-extremal linear pixels. For each of these regions, we proceed as in the proof of Proposition 2.2 by rewriting the evolution into a system of linear ODEs which has verbatim the same analytical solutions as before. Inspecting the proof of Proposition 2.2, one finds first that the proof of monotonicity preservation suffers no change at all. In the concavity preservation proof one finds that some of the summands of type $(f_{j-1} - 2f_j + f_{j+1})$ in the inequalities used there for $u_{k+1}(t) - 2u_k(t) + u_{k+1}(t)$ now vanish. However, for the entire right-hand side to vanish it is necessary that $(f_1 - C)$ and all $(f_{j-1} - 2f_j + f_{j+1})$ for $j = 1, \ldots, k$ are zero. This is true if and only if f_k itself is extremal. Consequently, under the evolution of the linear system, non-extremal pixels which are linear at $t = 0$ become convex if $\sigma_k = +1$ or concave if $\sigma_k = -1$ for any positive t. □

3 Time Discretisation

3.1 Explicit Time Discretisation

In the following we discuss time discretisations of our time-continuous system. We denote the time step by $\tau > 0$. A straightforward explicit time discretisation of our Problem then reads as follows:

Time-Discrete Problem. *Let $(\ldots, u_0^l, u_1^l, u_2^l, \ldots)$, $l = 0, 1, 2, \ldots$ be a series of bounded real-valued signals which satisfy the equations*

$$\frac{u_i^{l+1} - u_i^l}{\tau} = \begin{cases} \max(u_{i+1}^l - u_i^l, u_{i-1}^l - u_i^l, 0) \;, & 2u_i^l > u_{i+1}^l + u_{i-1}^l \;, \\ \min(u_{i+1}^l - u_i^l, u_{i-1}^l - u_i^l, 0) \;, & 2u_i^l < u_{i+1}^l + u_{i-1}^l \;, \\ 0 \;, & 2u_i^l = u_{i+1}^l + u_{i-1}^l \end{cases} \tag{9}$$

with the initial conditions

$$u_i^0 = f_i \;. \tag{10}$$

Assume further that the signal is either of infinite length or finite with reflecting boundary conditions.

Theorem 3.1 (Time-Discrete Well-Posedness) *Assume that in the Time-Discrete Problem the equality $f_{k+1} - 2f_k + f_{k-1} = 0$ does not hold for any pixel f_k which is not a local maximum or minimum of f. Assume further that $\tau < 1/2$. Then the statements of Theorem 2.1 are valid for the solution of the Time-Discrete Problem if only $u_k(t)$ for $t > 0$ is replaced everywhere by u_k^l with $l = 0, 1, 2, \ldots$*

The existence and uniqueness of the solution of the Time-Discrete Problem for $l = 0, 1, 2, \ldots$ is obvious. Maximum–minimum principle, l_∞-stability, total variation preservation and the steady state property are immediate consequences of the following proposition. It states that for $\tau < 1/2$ all qualitative properties of the time-continuous solution transfer to the time-discrete case.

Proposition 3.2 (Time-Discrete Solution) *Let u_i^l be the value of pixel i in time step l of the solution of our Time-Discrete Problem with time step size $\tau < 1/2$. Then the following hold for all $l = 0, 1, 2, \ldots$:*

(i) If u_1^l is a local maximum of u^l, then u_1^{l+1} is a local maximum of u^{l+1}.

(ii) If u_1^l is a concave pixel neighbouring to a convex pixel $u_0^l > u_1^l$, then u_1^{l+1} is again concave and has a convex neighbour pixel $u_0^{l+1} > u_1^{l+1}$.

(iii) If the segment $(u_1^l, \ldots, u_m^l)$ is strictly decreasing and concave in all pixels, and u_1^l is either a local maximum of u^l or neighbours to a convex pixel $u_0^l > u_1^l$, then the segment $(u_1^{l+1}, \ldots, u_m^{l+1})$ is strictly decreasing.

(iv) Under the same assumptions as in (iii), the segment $(u_1^{l+1}, \ldots, u_m^{l+1})$ is strictly concave in all pixels.

(v) If $2u_i^l = u_{i+1}^l + u_{i-1}^l$ holds for no pixel i, then $2u_i^{l+1} = u_{i+1}^{l+1} + u_{i-1}^{l+1}$ also holds for no pixel i.

(vi) Under the assumptions of (iii), all pixels in the range $i \in \{1, \ldots, m\}$ have the same limit $\lim\limits_{l\to\infty} u_i^l = C$ with $C := u_1^l$ if u_1^l is a local maximum, or $C := \frac{1}{2}(u_0^l + u_1^l)$ if it neighbours to the convex pixel u_0^l.

Analogous statements hold for local minima, for increasing concave and for convex signal segments.

Proof. Assume first that u_1^l is a local maximum of u^l. From the evolution equation (9) it is clear that $u_j^{l+1} \leq u_j^l + \tau(u_1^l - u_j^l)$ for $j = 0, 2$. For $\tau < 1$ this entails $u_j^{l+1} < u_1^l = u_1^{l+1}$, thus (i).

If instead u_1^l is a concave neighbour of a convex pixel $u_0^l > u_1^l$, then we have $u_1^{l+1} = u_1^l + \tau(u_0^l - u_1^l)$ and $u_0^{l+1} = u_0^l + \tau(u_1^l - u_0^l)$. Obviously, $u_0^{l+1} > u_1^{l+1}$ holds if and only if $\tau < 1/2$. For concavity, note that $u_2^{l+1} \leq u_2^l + \tau(u_1^l - u_2^l)$ and therefore $u_0^{l+1} - 2u_1^{l+1} + u_2^{l+1} \leq (1-\tau)(u_0^l - 2u_1^l + u_2^l) + 2\tau(u_1^l - u_0^l)$. The right-hand side is certainly negative for $\tau \leq 1/2$. An analogous argument secures convexity at pixel 0 which completes the proof of (ii).

In both cases we have $u_1^{l+1} \geq u_1^l$. Under the assumptions of (iii), (iv) we then have $u_k^{l+1} = u_k^l + \tau(u_{k-1}^l - u_k^l)$ for $k = 2, \ldots, m$. If $\tau < 1$, it follows that $u_k^l < u_k^{l+1} \leq u_{k-1}^l$ for $k = 2, \ldots, m$ which together with $u_1^{l+1} \geq u_1^l$ implies that $u_{k-1}^{l+1} > u_k^l$ for $k = 2, \ldots, m$ and therefore (iii).

For the concavity condition we compute

$$u_{k-1}^{l+1} - 2u_k^{l+1} + u_{k+1}^{l+1} = (1-\tau)(u_{k-1}^l - 2u_k^l + u_{k+1}^l) + \tau(u_{k-2}^l - 2u_{k-1}^l + u_k^l)$$

for $k = 3, \ldots, m-1$. The right-hand side is certainly negative for $\tau \leq 1$ which secures concavity in the pixels $k = 3, \ldots, m-1$. Concavity in pixel m for $\tau \leq 1$ follows from essentially the same argument. However, the equation is now replaced by an inequality since for pixel $m+1$ we know only that $u_{m+1}^{l+1} \leq u_{m+1}^l + \tau(u_m^l - u_{m+1}^l)$. If u_1^l is a local maximum and therefore $u_1^{l+1} = u_1^l$, we find for pixel 2 that $u_1^{l+1} - 2u_2^{l+1} + u_3^{l+1} = (1-\tau)(u_1^l - 2u_2^l + u_3^l) + \tau(u_2^l - u_1^l)$ which again secures concavity for $\tau \leq 1$. As was proven above, concavity in pixel 1 is preserved for $\tau \leq 1/2$ such that (iv) is proven.

Under the hypothesis of (v), the evolution of all pixels in the signal is described by statements (i)–(iv) or their obvious analoga for increasing and convex segments. The claim of (v) then is obvious.

Finally, addition of the equalities $C - u_1^{l+1} = (1-2\tau)(C - u_1^l)$ and $u_{i-1}^{l+1} - u_i^{l+1} = (1-\tau)(u_{i-1}^l - u_i^l)$ for $i = 2, \ldots, m$ implies that

$$C - u_k^{l+1} = (1-\tau)(C - u_k^l) - \tau(C - u_1^l) < (1-\tau)(C - u_k^l)$$

for all $k = 1, \ldots, m$. By induction, we have

$$C - u_k^{l+l'} \leq (1-\tau)^{l'}(C - u_k^l)$$

where the right-hand side tends to zero for $l' \to \infty$. Together with the monotonicity preservation for $\tau < 1/2$, statement (vi) follows. □

We remark that in the presence of non-extremal linear pixels, uniqueness fails in a similar way as in the semidiscrete setting.

3.2 Modified Explicit Time Discretisation

A closer look at the proof of Proposition 3.2 reveals that the limitation $\tau < 1/2$ is made necessary only by the situation of case (ii) of the proposition, i.e. a concave pixel following a convex one within a decreasing segment, or symmetrical situations. In the absence of such a configuration, the statements hold even for all $\tau < 1$.

By a small adaptation of the time-discrete evolution rule we can therefore obtain a scheme which satisfies well-posedness properties for time step sizes up to 1.

Modified Time-Discrete Problem. *Let $(\ldots, u_0^l, u_1^l, u_2^l, \ldots)$, $l = 0, 1, 2, \ldots$ be a series of bounded real-valued signals which is generated by the equations*

$$\frac{\tilde{u}_i^l - u_i^l}{\tau} = \begin{cases} \max(u_{i+1}^l - u_i^l, u_{i-1}^l - u_i^l, 0)\ , & 2u_i^l > u_{i+1}^l + u_{i-1}^l\ , \\ \min(u_{i+1}^l - u_i^l, u_{i-1}^l - u_i^l, 0)\ , & 2u_i^l < u_{i+1}^l + u_{i-1}^l\ , \\ 0\ , & 2u_i^l = u_{i+1}^l + u_{i-1}^l\ , \end{cases} \tag{11}$$

$$u_i^{l+1} = \begin{cases} \frac{1}{2}(\tilde{u}_{i+1}^l + \tilde{u}_i^l)\ , & (\tilde{u}_{i+1}^l - \tilde{u}_i^l)(u_{i+1}^l - u_i^l) < 0\ , \\ \frac{1}{2}(\tilde{u}_{i-1}^l + \tilde{u}_i^l)\ , & (\tilde{u}_{i-1}^l - \tilde{u}_i^l)(u_{i-1}^l - u_i^l) < 0\ , \\ \tilde{u}_i^l\ , & \textit{else} \end{cases} \tag{12}$$

with the initial conditions (10) *and boundary conditions as in the previous Time-Discrete Problem.*

Note that the case distinction on the right-hand side of (12) is sound since the case (ii) of Proposition 3.2 cannot occur simultaneously on both sides of the same pixel. Further, it is clear from Proposition 3.2 that the Modified Time-Discrete Problem is identical with the Time-Discrete Problem for $\tau < 1/2$.

For the Modified Time-Discrete Problem, the well-posedness statements of Theorem 3.1 hold for all $\tau \le 1$. Since the proof contains only slight modifications compared to the previous one, we do not repeat it here but state only the suitably modified version of Proposition 3.2. The main modification is that *extremal* linear pixels can now arise during the evolution.

Proposition 3.3 (Modified Time-Discrete Solution) *Let u_i^l be the value of pixel i in time step l of the solution of our Modified Time-Discrete Problem with time step size $\tau \le 1$. Then the following hold for all $l = 0, 1, 2, \ldots$:*

(i) If u_1^l is a local maximum of u^l, then u_1^{l+1} is a local maximum of u^{l+1}.

(ii) If u_1^l is a concave pixel neighbouring to a convex pixel $u_0^l > u_1^l$, then u_1^{l+1} is again concave and has a convex neighbour pixel $u_0^{l+1} \ge u_1^{l+1}$.

(iii) If the segment $(u_1^l, \ldots, u_m^l)$ is strictly decreasing and concave in all pixels, and u_1^l is either a local maximum of u^l or neighbours to a convex pixel $u_0^l > u_1^l$, then the segment $(u_2^{l+1}, \ldots, u_m^{l+1})$ is strictly decreasing, and $u_1^{l+1} \ge u_2^{l+1}$.

(iv) Under the same assumptions as in (iii), the segment $(u_2^{l+1}, \ldots, u_m^{l+1})$ is strictly concave in all pixels. Pixel u_1^{l+1} is strictly concave except if u_1^l is a local maximum, and $\tau = 1$.

(v) If $2u_i^l = u_{i+1}^l + u_{i-1}^l$ holds for no pixel i for which $u_{i-1}^l = u_i^l = u_{i+1}^l$ does not hold, then $2u_i^{l+1} = u_{i+1}^{l+1} + u_{i-1}^{l+1}$ also holds for no pixel i for which $u_{i-1}^{l+1} = u_i^{l+1} = u_{i+1}^{l+1}$ does not hold.

(vi) Under the assumptions of (iii), all pixels in the range $i \in \{1, \ldots, m\}$ have the same limit $\lim_{l \to \infty} u_i^l = C$ with $C := u_1^l$ if u_1^l is a local maximum, or $C := \frac{1}{2}(u_0^l + u_1^l)$ if it neighbours to the convex pixel u_0^l.

Analogous statements hold for local minima, for increasing concave and for convex signal segments.

The special case $\tau = 1$ deserves a closer consideration. Straightforward calculations reveal that a pixel neighbouring to a local maximum attains the same value as the maximum in the next time step. Moreover, a pair of a convex pixel followed by a concave one in a decreasing segment aligns to equal values within one time step, turning both pixels into discrete local extrema. These facts give rise to the following corollary.

Corollary 3.4 *Consider the Modified Time-Discrete Problem with $\tau = 1$. If at time step $k = l$ the segment $(u_1^l, u_2^l, \ldots, u_m^l)$ has the properties required in Prop. 3.3, (iii), then each pixel u_k of this segment becomes constant after not more than k time steps.*

In the case of finite-length signals, or infinite signals in which there exists a finite upper bound to the length of monotonic concave or convex segments, this corollary implies that the steady state is reached in finite time.

Since the modified time-discrete filter propagates grey-values in x direction one pixel per time step, it turns out to reflect particularly well the behaviour of dilations and erosions on a continuous domain. In the light of our remark at the end of Subsection 2.2, it can be said that the approximation error introduced by spatial discretisation has been compensated exactly by the time discretisation.

A further view on the modified scheme is that it can be related to *locally analytic schemes.* Schemes of this type compose analytic solutions for certain dynamical systems in a neighbourhood of each location into approximate solutions on the entire grid. Examples are the numerical scheme for 1-D total variation (TV) flow introduced in [15, Sec. 4.2] which relies on analytic solutions for TV flow on two pixels, or its 2-D extension set forth in [21] which is based on four-pixel systems.

Our modified time-discrete shock filtering scheme can be understood as a locally analytic scheme built on the analytical solutions (for $0 \leq \tau \leq 1$) of *space-continuous* dilation and erosion filters where the signal is linearly interpolated between subsequent pixels.

4 Equivalence to Local Mode Filtering

Now that we have derived well-posedness properties for semidiscrete and fully discrete shock filters, let us also establish an equivalence result between shock filters and a class of discrete filters based on local signal statistics, namely so-called mode filters.

Discrete filters exploiting local signal statistics evaluate signal values from a sliding window neighbourhood to determine a new value for each pixel. Commonly used representatives of this class are box-average filters, median filters and generally M-smoothers, but also discrete dilation and erosion.

One statistical parameter of the local greyvalue distribution that is not used in one of the aforementioned filters is the *mode*. The mode of a continuous distribution is defined as its most probable value. Analogous as above, determining the mode of the grey-values within a sliding window or structuring element constitutes a local mode filter for images [3, 16, 5].

However, applying this procedure to spatially discretised signals faces a problem because the distribution is now given only by finitely many values. Defining the mode simply as the most frequent value is not helpful since in generic cases there are no duplicates among the values.

Instead, we combine a polynomial approximation with local histogram properties to find the mode value within a sliding window containing three pixels.

Assume we have a one-dimensional discrete signal $(\ldots, u_0^l, u_1^l, u_2^l, \ldots)$. By our sliding window we select three subsequent values $u_{i-1}^l, u_i^l, u_{i+1}^l$. The value at pixel i of the signal filtered by our local mode filter should be the mode value of $u_{i-1}^l, u_i^l, u_{i+1}^l$.

To begin with, we interpolate by a quadratic polynomial through the three points $(i-1, u_{i-1}^l)$, (i, u_i^l), $(i+1, u_{i+1}^l)$. Translating, for simplicity, spatial coordinates by $-i$, we therefore want the quadratic polynomial

$$p(z) = az^2 + bz + c$$

to satisfy the conditions

$$p(-1) = u_{i-1}^l \ , \quad p(0) = u_i^l \ , \quad p(1) = u_{i+1}^l \ .$$

This gives the system of three equations

$$\begin{aligned} a - b + c &= u_{i-1}^l \ , \\ c &= u_i^l \ , \\ a + b + c &= u_{i+1}^l \ , \end{aligned}$$

with the solution

$$a = \frac{u_{i-1}^l - 2u_i^l + u_{i+1}^l}{2} \ , \quad b = \frac{u_{i+1}^l - u_{i-1}^l}{2} \ , \quad c = u_i^l \ .$$

Having determined $p(z)$, we are now interested in the location of the mode of its values. First, if $a = 0$, p is a linear polynomial whose values are uniformly distributed. In this case, we have our local mode filter not change the value of pixel i.

If $a \neq 0$, the density of the distribution of values of p attains its maximum at the (uniquely determined) stationary value of p. The extremum of $p(z)$ is located at

$$-\frac{b}{2a} = \frac{u_{i-1}^l - u_{i+1}^l}{u_{i-1}^l - 2u_i^l + u_{i+1}^l} =: e \ .$$

However, whenever $e \notin \{-1, 0, +1\}$, the extremal value $p(e)$ will lie outside the interval $I_i := [\min(u_{i-1}^l, u_i^l, u_{i+1}^l), \max(u_{i-1}^l, u_i^l, u_{i+1}^l)]$; choosing $p(e)$ as the value of the mode filter therefore results in over- and undershoots.

This leads us to stabilise our filtering procedure by projecting $p(e)$ to the interval I_i, i.e. *choosing as the new value of pixel i the value from the interval I_i which is closest to $p(e)$.* We will call this procedure *stabilised discrete local mode filtering.* Clearly, for p not linear this filter will always return as its value one of the end points of I_i, namely $\min(u_{i-1}^l, u_i^l, u_{i+1}^l)$ if $a < 0$, or $\max(u_{i-1}^l, u_i^l, u_{i+1}^l)$ if $a > 0$.

We have therefore arrived at the following equivalence result.

Proposition 4.1 *Stabilised discrete local mode filtering of a 1-D discrete signal* $(\ldots, f_0, f_1, f_2, \ldots)$ *obeys the equation*

$$u_i = \begin{cases} \min(u_{i-1}^l, u_i^l, u_{i+1}^l) \;, & u_{i-1}^l - 2u_i^l + u_{i+1}^l < 0 \;, \\ \max(u_{i-1}^l, u_i^l, u_{i+1}^l) \;, & u_{i-1}^l - 2u_i^l + u_{i+1}^l > 0 \;, \\ u_i^l \;, & u_{i-1}^l - 2u_i^l + u_{i+1}^l = 0 \;. \end{cases}$$

Consequently, it is equivalent to one step of time-discrete shock filtering as described in Subsection 3.1 with time step size $\tau = 1$.

Since the time step size $\tau = 1$ exceeds the limit given in Theorem 3.1, the well-posedness properties do not transfer fully to stabilised discrete local mode filtering. However, a modification along the line of Section 3.2 could also be applied to local mode filtering to obtain a well-posed process.

5 Conclusions

Theoretical foundation for PDE-based shock filtering has long been considered to be a hopelessly difficult problem. In this paper we have shown that it is possible to obtain both an analytical solution and well-posedness by considering the space-discrete case where the partial differential equation becomes a dynamical system of ordinary differential equations (ODEs). Corresponding results can also be established in the fully discrete case when an explicit time discretisation is applied to this ODE system. Last but not least, we were able to derive equivalence results between shock filtering and local mode filtering.

Since local mode filtering also satisfies equivalence properties to robust estimation and mean shift analysis [17], it becomes clear that shock filtering is much more than a simple image enhancement method: It is a theoretically well-founded class of methods that can be justified in many different ways.

We are convinced that the basic idea in our paper, namely to establish well-posedness results for difficult PDEs in image analysis by considering the semidiscrete case, is also useful in a number of other important PDEs. While this has already been demonstrated for nonlinear diffusion filtering [18, 12], we plan to investigate a number of other PDEs in this manner, both in the one- and the higher-dimensional case. This should give important theoretical insights into the dynamics of these experimentally well-performing nonlinear processes.

References

[1] L. Alvarez and L. Mazorra. Signal and image restoration using shock filters and anisotropic diffusion. *SIAM Journal on Numerical Analysis*, 31:590–605, 1994.

[2] R. W. Brockett and P. Maragos. Evolution equations for continuous-scale morphology. In *Proc. IEEE International Conference on Acoustics, Speech and Signal Processing*, volume 3, pages 125–128, San Francisco, CA, Mar. 1992.

[3] G. B. Coleman and H. C. Andrews. Image segmentation by clustering. *Proceedings of the IEEE*, 67(5):773–785, May 1979.

[4] G. Gilboa, N. A. Sochen, and Y. Y. Zeevi. Regularized shock filters and complex diffusion. In A. Heyden, G. Sparr, M. Nielsen, and P. Johansen, editors, *Computer Vision – ECCV 2002*, volume 2350 of *Lecture Notes in Computer Science*, pages 399–413. Springer, Berlin, 2002.

[5] L. D. Griffin. Mean, median and mode filtering of images. *Proceedings of the Royal Society of London, Series A*, 456(2004):2995–3004, 2000.

[6] F. Guichard and J.-M. Morel. A note on two classical shock filters and their asymptotics. In M. Kerckhove, editor, *Scale-Space and Morphology in Computer Vision*, volume 2106 of *Lecture Notes in Computer Science*, pages 75–84. Springer, Berlin, 2001.

[7] P. Kornprobst, R. Deriche, and G. Aubert. Nonlinear operators in image restoration. In *Proc. 1997 IEEE Computer Society Conference on Computer Vision and Pattern Recognition*, pages 325–330, San Juan, Puerto Rico, June 1997. IEEE Computer Society Press.

[8] H. P. Kramer and J. B. Bruckner. Iterations of a non-linear transformation for enhancement of digital images. *Pattern Recognition*, 7:53–58, 1975.

[9] S. Osher and L. Rudin. Shocks and other nonlinear filtering applied to image processing. In A. G. Tescher, editor, *Applications of Digital Image Processing XIV*, volume 1567 of *Proceedings of SPIE*, pages 414–431. SPIE Press, Bellingham, 1991.

[10] S. Osher and L. I. Rudin. Feature-oriented image enhancement using shock filters. *SIAM Journal on Numerical Analysis*, 27:919–940, 1990.

[11] S. Osher and J. A. Sethian. Fronts propagating with curvature-dependent speed: Algorithms based on Hamilton–Jacobi formulations. *Journal of Computational Physics*, 79:12–49, 1988.

[12] I. Pollak, A. S. Willsky, and H. Krim. Image segmentation and edge enhancement with stabilized inverse diffusion equations. *IEEE Transactions on Image Processing*, 9(2):256–266, Feb. 2000.

[13] L. Remaki and M. Cheriet. Numerical schemes of shock filter models for image enhancement and restoration. *Journal of Mathematical Imaging and Vision*, 18(2):153–160, Mar. 2003.

[14] J. G. M. Schavemaker, M. J. T. Reinders, J. J. Gerbrands, and E. Backer. Image sharpening by morphological filtering. *Pattern Recognition*, 33:997–1012, 2000.

[15] G. Steidl, J. Weickert, T. Brox, P. Mrázek, and M. Welk. On the equivalence of soft wavelet shrinkage, total variation diffusion, total variation regularization, and SIDEs. *SIAM Journal on Numerical Analysis*, 42(2):686–713, 2004.

[16] P. L. Torroba, N. L. Cap, H. J. Rabal, and W. D. Furlan. Fractional order mean in image processing. *Optical Engineering*, 33(2):528–534, Feb. 1994.

[17] R. van den Boomgaard and J. van de Weijer. On the equivalence of local-mode finding, robust estimation and mean-shift analysis as used in early vision tasks. In *Proc. 16th*

International Conference on Pattern Recognition, volume 3, pages 927–930, Quebec City, Canada, Aug. 2002.

[18] J. Weickert. *Anisotropic Diffusion in Image Processing.* Teubner, Stuttgart, 1998.

[19] J. Weickert. Coherence-enhancing shock filters. In B. Michaelis and G. Krell, editors, *Pattern Recognition*, volume 2781 of *Lecture Notes in Computer Science*, pages 1–8, Berlin, 2003. Springer.

[20] M. Welk and J. Weickert. Semidiscrete and discrete well-posedness of shock filtering. In C. Ronse, L. Najman, and E. Decencière, editors, *Mathematical Morphology: 40 Years On*, volume 30 of *Computational Imaging and Vision*, pages 311–320. Springer, Dordrecht, 2005.

[21] M. Welk, J. Weickert, and G. Steidl. A four-pixel scheme for singular differential equations. In R. Kimmel, N. Sochen, and J. Weickert, editors, *Scale-Space and PDE Methods in Computer Vision*, volume 3459 of *Lecture Notes in Computer Science*, pages 585–597, Berlin, 2005. Springer.